

## Stability of analog neural networks with delay

C. M. Marcus and R. M. Westervelt

*Division of Applied Sciences and Department of Physics, Harvard University, Cambridge, Massachusetts 02138*

(Received 11 August 1988)

Continuous-time analog neural networks with symmetric connections will always converge to fixed points when the neurons have infinitely fast response, but can oscillate when a small time delay is present. Sustained oscillation resulting from time delay is relevant to hardware implementations of neural networks where delay due to the finite switching speed of amplifiers can be appreciable compared to the network relaxation time. We analyze the dynamics of continuous-time analog networks with delay, and show that there is a critical delay above which a symmetrically connected network will oscillate. Two different stability analyses are presented for low and high neuron gain. The results are useful as design criteria for building fast but stable electronic networks. We find that for some connection topologies, a delay much smaller than the relaxation time can lead to oscillation, whereas for other topologies, including associative memory networks, even long delays will not produce oscillation. The most oscillation-prone network configuration is the all-inhibitory network; in this configuration, the critical delay for oscillation is smaller than the network relaxation time by a factor of  $N$ , the size of the network. Theoretical results are compared with numerical simulations and with experiments performed on a small (eight neurons) electronic network with controllable delay.

### I. INTRODUCTION

Much of the current interest in artificial networks stems not only from their richness as a theoretical model of collective dynamics but also from the promise they have shown as a practical tool for performing parallel computation.<sup>1</sup> Theoretical understanding of neural-network dynamics has advanced greatly in the past few years.<sup>2-7</sup> At the same time, electronic implementations of analog neural networks in very-large-scale integration (VLSI) technology have begun to appear.<sup>1,8</sup> As these two lines of research converge, it becomes important to understand the applicability of theoretical results to hardware neural networks. Hardware realities such as switching delays, parameter variability, and parasitic capacitances and inductances, which are frequently neglected in idealized models, can lead to instabilities not predicted by theory. Our current understanding of network dynamics must be extended to more realistic conditions in order to produce useful, stable, and fast microelectronic neural networks.

It is well known that symmetrically connected networks of analog neurons operating in continuous time will not oscillate.<sup>4,5</sup> However, this result assumes that neurons communicate and respond instantaneously. In electronic neural networks, time delays will be present due to the finite switching speed of amplifiers. Designing a network to operate more quickly will increase the relative size of the intrinsic delay and can eventually lead to oscillation. In biological neural networks it is known that time delay can cause an otherwise stable system to oscillate.<sup>9-12</sup> Instabilities introduced by delays have also been analyzed in the context of control theory and electrical engineering.<sup>13</sup> Neural-network models with two-state neurons operating in discrete time with parallel up-

date dynamics are also known to oscillate.<sup>2,14-17</sup> These networks correspond to the infinite-gain and infinite-delay limits of the model presented in Sec. II.

In this paper, we show how the existence of oscillatory modes in continuous-time analog neural networks with time delay depends on the neuron gain and delay and on the size and connection topology of the network. We find that for certain connection topologies, delays much less than the network relaxation time can lead to sustained oscillation, while for other network topologies, even long delays (compared to the relaxation time) will not induce oscillation. For those network configurations which can oscillate for small delay, we find the critical value of delay below which the network will not support sustained oscillation. This critical delay depends on the gain of the neurons and the eigenvalues of the connection matrix.

The aim of this paper is to provide a design criterion for building stable analog networks, extending the criterion: "symmetric connections implies no oscillation" to the case of analog networks with time delay. Our results are based on local rather than global stability analysis and therefore do not provide a rigorous guarantee of stability. Rather, we support our results with numerical and experimental evidence suggesting that the stability criteria presented here are valid under the conditions investigated. In addition to using numerical integration to test the theoretical results, we have measured critical delays and basins of attraction for sustained oscillation in a small (eight neurons) electronic network with controllable time delay based on charge-coupled device circuitry.<sup>18</sup>

In Sec. II we derive a general system of delay-differential equations starting from the circuit equations for an electronic network and describe the simplifying assumptions of our model. In Sec. III we present a linear

stability analysis about the point where all neurons have zero input and steepest transfer function. This point is defined as the origin of an  $N$ -dimensional space where each direction represents the input voltage of a neuron. For sufficiently large neuron gain, the origin loses stability in either a pitchfork bifurcation, which creates fixed points away from the origin, or in a Hopf bifurcation<sup>19</sup> which creates an attractor for sustained oscillation. Which sort of bifurcation occurs first depends on the largest and smallest eigenvalues of the connection matrix and on the normalized delay. Experimentally, we find that the Hopf bifurcation marks the appearance of sustained oscillation in symmetric networks. The analysis in Sec. III is formulated as a design criterion that will yield fixed-point dynamics in a delay network as long as the ratio of delay to relaxation time is kept below a critical value.

In Sec. IV we consider networks operating in a large-gain regime where fixed-point attractors away from the origin and oscillatory attractors coexist, each with large basins of attraction.<sup>18</sup> We restrict our attention in this regime to networks which oscillate coherently. We find experimentally that the size of the basin of attraction for coherent oscillation depends on the time delay, decreasing in size as the delay is reduced. At a critical value of delay the coherent oscillatory attractor disappears, and only fixed-point attractors are observed. We present a novel nonlinear stability analysis of the coherent oscillatory attractor which yields a critical delay for sustained oscillation in these networks.

The results of the linear and nonlinear stability analyses presented in Secs. III and IV are compared with numerical integration of the delay-differential equations and experiments in the eight-neuron electronic delay network; good agreement is found between theory, experiment, and numerics.

In Sec. V we discuss stability for three specific network topologies: symmetric rings of neurons, symmetric random networks, and associative memory networks based on the Hebb rule.<sup>20</sup> A particularly important result is that Hebb rule networks are stable for long delays, but that clipping algorithms which limit the connection strengths to a few values can yield an interconnection matrix with large negative eigenvalues which can lead to sustained oscillation. Finally, a summary of useful results is given in Sec. VI.

## II. DYNAMICAL EQUATIONS FOR ANALOG NETWORKS WITH DELAY

In this section we derive a general system of delay-differential equations, Eq. (2.3), starting from the circuit equations for a network of  $N$  saturating voltage amplifiers ("neurons") with delayed output coupled via a resistive interconnection matrix. The circuit is the same as the analog network described by Hopfield in Ref. 4, with the addition of a delay  $\tau'$ ,

$$C_i \dot{u}_i(t') = -\frac{1}{R_i} u_i(t') + \sum_{j=1}^N T_{ij} f_j(u_j(t' - \tau'_j)) . \quad (2.1)$$

The variable  $u_i(t')$  represents the voltage on the input of the  $i$ th neuron. Each neuron is characterized by an input capacitance  $C_i$ , a delay  $\tau'_i$ , and a transfer function  $f_i$ . The nonlinear transfer function  $f(u)$  is sigmoidal, saturating at  $\pm 1$  with maximum slope at  $u = 0$ . The connection matrix element  $T_{ij}$  has a value  $+1/R_{ij}$  when the noninverting output of  $j$  is connected to the input of  $i$  through a resistance  $R_{ij}$ , and a value  $-1/R_{ij}$  when the inverting output of  $j$  is connected to the input of  $i$  through a resistance  $R_{ij}$ . The parallel resistance at the input of each neuron is defined  $R_i = (\sum_j |T_{ij}|)^{-1}$ . We consider the case of identical neurons  $C_i = C$ ,  $f_i = f$ ,  $\tau'_i = \tau'$  and also assume that each neuron is connected to the same total input resistance, defining  $R = R_i$  for all  $i$ . With these assumptions, the equations of motion become

$$RC \dot{u}_i(t') = -u_i(t') + R \sum_{j=1}^N T_{ij} f(u_j(t' - \tau')) . \quad (2.2)$$

Rescaling time, delay, and  $T_{ij}$  gives the following new variables:  $t = t'/RC$ ,  $\tau = \tau'/RC$ ,  $J_{ij} = RT_{ij}$ . This definition of  $J_{ij}$  has a normalization  $\sum_j |J_{ij}| = 1$ . In terms of these scaled variables the delay system takes on the simple and general form

$$\dot{u}_i(t) = -u_i(t) + \sum_{j=1}^N J_{ij} f(u_j(t - \tau)) . \quad (2.3)$$

All times in Eq. (2.3) are in units of the characteristic network relaxation time  $RC$ .

The initial conditions for a delay-differential system must be specified as a function  $\phi_i$ :  $[-\tau, 0]$ . All experimental and numerical results presented take each  $\phi_i$  to be constant on the interval  $[-\tau, 0]$ , though not necessarily the same for different  $i$ . A cursory numerical investigation suggests that the stability results presented below do not depend on the particulars of the initial function  $\phi_i$ .

## III. LINEAR STABILITY ANALYSIS OF DELAY NETWORKS

We consider the stability of Eq. (2.3) near the origin ( $u_i = 0$  for all  $i$ ). Linearizing  $f_i(u)$  gives

$$\dot{u}_i(t) = -u_i(t) + \sum_{j=1}^N \beta J_{ij} u_j(t - \tau) , \quad (3.1)$$

where the gain  $\beta$  is defined as slope of  $f_i(u)$  at  $u = 0$ . It is convenient to represent the linearized system of  $N$  delay equations as amplitudes  $x_i$  ( $i = 1, \dots, N$ ) along the  $N$  eigenvectors of the connection matrix  $J_{ij}$ ,

$$\dot{x}_i(t) = -x_i(t) + \beta \lambda_i x_i(t - \tau) , \quad (3.2)$$

where  $\lambda_i$  ( $i = 1, \dots, N$ ) are the eigenvalues of the connection matrix  $J_{ij}$ . The  $\lambda_i$  will be referred to as the connection eigenvalues to avoid confusion with the roots of the characteristic equation which will be derived from Eq. (3.2). In general these connection eigenvalues are complex; when  $J_{ij}$  is a symmetric matrix, the  $\lambda_i$  are real. Assuming exponential time evolution of the  $x_i$ , we introduce the complex characteristic exponents  $s_i$  and define

$x_i(t) = x_i(0)e^{s_i t}$ . Substituting this form of  $x_i(t)$  into Eq. (3.2) gives the characteristic equation

$$(s_i + 1)e^{s_i \tau} = \beta \lambda_i. \quad (3.3)$$

The origin is asymptotically stable when  $\text{Re}(s_i) < 0$  for all  $i$ .<sup>21</sup> When  $\text{Re}(s_k) > 0$  for some  $k$ , the origin is unstable to perturbations in the direction of the eigenvector associated with  $s_k$ .

#### A. Linear stability analysis with $\tau=0$

When the neurons have zero delay ( $\tau=0$ ) Eq. (3.3) reduces to  $(s_i + 1) = \beta \lambda_i$ . In this case the origin is the unique attractor as long as all connection eigenvalues  $\lambda_i$  have real part less than  $1/\beta$  as shown in Fig. 1. For a symmetric connection matrix, the  $\lambda_i$  are real and the bifurcation is of the pitchfork type: For  $\beta > 1/\lambda_k$  the origin becomes a saddle and a pair of stable fixed points appears on opposite sides of the origin in the direction of the  $k$ th eigenvector of  $J_{ij}$ . In neural networks language, this new pair of fixed points away from the origin is a memory.

As an example of linear stability analysis with  $\tau=0$ , consider the  $N \times N$  all-excitatory or ferromagnetic interaction matrix ( $T_{ij} = +1/R$ ;  $T_{ii} = 0$ )

$$J_{ij} = \frac{1}{N-1} \begin{pmatrix} 0 & 1 & 1 & \cdots & 1 \\ 1 & 0 & 1 & & 1 \\ 1 & 1 & 0 & & 1 \\ \cdots & & & \cdots & \\ 1 & 1 & 1 & \cdots & 0 \end{pmatrix}. \quad (3.4)$$

The connection eigenvalues for this matrix are

$$\lambda_i = \begin{cases} 1 & \text{(once)} \\ -1/(N-1) & \text{(} N-1 \text{ degenerate)}. \end{cases} \quad (3.5)$$

Notice that because  $J_{ij}$  is symmetric the  $\lambda_i$  are real.

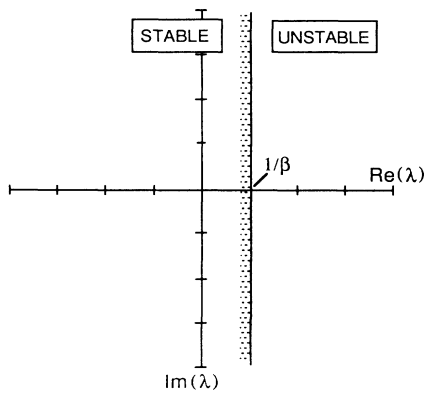


FIG. 1. The stability of the origin for zero delay is determined by the condition  $\text{Re}(\lambda_i) < 1/\beta$  for all  $i$ , where  $\lambda_i$  are the eigenvalues of the connection matrix  $J_{ij}$  that appears in Eq. (2.3). The border of the stability region is shown as a vertical line in the complex  $\lambda$  plane.

When  $\beta < 1/\lambda_{\max}$  where  $\lambda_{\max}$  is the maximum connection eigenvalue, the origin is the only attractor. When  $\beta > 1/\lambda_{\max}$  the origin is unstable, and two fixed points appear on either side of the origin in the eigenvector associated with  $\lambda_{\max}$ . In this case  $\lambda_{\max} = 1$  from Eq. (3.5) and the eigenvector associated with  $\lambda_{\max}$  is the ferromagnetic direction ( $u_i = 1$  for all  $i$ ).

A second example is the  $N \times N$  all-inhibitory or antiferromagnetic connection matrix

$$J_{ij} = \frac{1}{N-1} \begin{pmatrix} 0 & -1 & -1 & \cdots & -1 \\ -1 & 0 & -1 & & -1 \\ -1 & -1 & 0 & & -1 \\ \cdots & & & \cdots & \\ -1 & -1 & -1 & \cdots & 0 \end{pmatrix}. \quad (3.6)$$

This network configuration is important in neural networks as a model of lateral inhibition<sup>10</sup> and as a so-called winner-take-all circuit.

The eigenvalues for the all-inhibitory network are

$$\lambda_i = \begin{cases} 1/(N-1) & \text{(} N-1 \text{ degenerate)} \\ -1 & \text{(once)}. \end{cases} \quad (3.7)$$

For this network configuration, the origin does not become unstable, and fixed points away from the origin do not appear until  $\beta > 1/\lambda_{\max} = N-1$ . Thus the origin for a large all-inhibitory network is very stable for zero delay. The eigenvector associated the minimum eigenvector  $\lambda_{\min}$  is in the ferromagnetic direction ( $u_i = 1$  for all  $i$ ). The  $N-1$  eigenvectors associated with the degenerate  $\lambda_{\max}$  each satisfy the condition  $\sum_i u_i = 0$  which defines a hyperplane perpendicular to the ferromagnetic direction.

#### B. Frustration and equivalent networks

A symmetric matrix with connection strengths limited to three values—positive, negative, and zero—can be represented as an undirected signed graph with a neuron at each vertex.<sup>18</sup> An important property of the all-inhibitory network discussed above is that every loop formed from three neurons in the connection graph has an odd number of negative (inhibitory) edges. A connection graph containing loops with an odd number of negative edges is said to be frustrated. Frustration is important in systems with competing interactions<sup>22</sup> and is considered essential in the formation of spin-glass state in magnetic systems.<sup>23</sup> We suspect, though have not proven, that frustration is also essential for delay-induced oscillation when there is no self-connection, i.e.,  $J_{ii} = 0$ . Because every triangular loop in the all-inhibitory network has an odd number of negative edges, this configuration is said to be fully frustrated. There are  $2^{N-1}$  other networks that are also fully frustrated; these other configurations are related by the Mattis transformation:<sup>24</sup> For any  $i$  let  $u_i \rightarrow -u_i$  and  $J_{ij} \rightarrow -J_{ij}$  for all  $j$ . All  $2^{N-1}$  fully frustrated networks have identical dynamics up to changes of sign. Similarly, there are  $2^{N-1}$  networks equivalent to the ferromagnetic network, Eq. (3.4), all of which are completely unfrustrated.

### C. Linear stability analysis with delay

In this section we show that for  $\tau > 0$  the stability region, defined by the condition  $\text{Re}(s_j) < 0$ , is no longer a simple vertical line at  $1/\beta$  in the complex  $\lambda$  plane as in Fig. 1, but forms a closed teardrop-shaped region that becomes smaller and more circular as the delay is increased as shown in Fig. 2. This idea was discussed by May in Ref. 25. As  $\tau \rightarrow 0$ , the region of stability expands to fill the half-plane  $\text{Re}(\lambda) < 1/\beta$ , recovering Fig. 1. As  $\tau \rightarrow \infty$  the stability region becomes a circle centered at  $\lambda = 0$  with radius  $1/\beta$ . A circular stability region is characteristic of iterated map dynamics just as a half-plane stability region is characteristic of differential equation dynamics; thus as delay is increased from  $\tau \ll 1$  to  $\tau \gg 1$  the local stability condition of the delay-differential system goes from that of continuous-time, differential equation dynamics to iterated map or parallel-update dynamics.<sup>25</sup> The dynamics of a parallel-update network  $u_i(n+1) = \sum_j J_{ij} f(u_j(n))$ , where  $n$  is the index of discrete time, corresponds to the long-delay limit of Eq. (3.1). It is known that parallel update networks can oscillate with a symmetric connection matrix.<sup>2,14-17</sup> Sufficient conditions for which parallel-update networks will not oscillate have been presented.<sup>15-17</sup>

The exact shape of the stability region at any value of delay can be found by substituting  $s_j = \sigma_j + i\omega_j$  into Eq. (3.3) and finding the condition  $\sigma_j = 0$ . The loci of points on the border of the stability region can be written in polar coordinates as

$$\lambda_{\text{border}} = \Lambda(\theta)e^{i\theta}, \quad (3.8)$$

where  $\Lambda(\theta) > 0$  is the radial distance from the origin  $\lambda = 0$  to the border at an angle  $\theta$  from the positive  $\text{Re}(\lambda)$  axis. Putting Eq. (3.8) and the condition  $\sigma_j = 0$  into Eq. (3.3) gives

$$(i\omega_j + 1)e^{i\omega_j\tau} = \beta\Lambda(\theta)e^{i\theta}. \quad (3.9)$$

Solving for  $\Lambda(\theta)$  gives the border of the stability region as an implicit function of delay:

$$\Lambda(\theta) = \frac{1}{\beta}(\omega_j^2 + 1)^{1/2}, \quad (3.10a)$$

$$-\omega_j = \tan(\omega_j\tau - \theta), \quad (3.10b)$$

where  $\omega_j$  is in the range  $(\theta - \pi/2) \leq \omega_j\tau \leq \theta \pmod{2\pi}$ . We are interested in the *smallest* root  $\omega_j$  of Eq. (3.10b) for a given value of  $\theta$  and  $\tau$ . Large roots of Eq. (3.10b) produce large values of  $\Lambda(\theta)$  by Eq. (3.10a), which lie outside of the stability region defined by the smaller roots. Only the part of the  $\lambda$  plane inside the smallest stability region is actually stable. The stability region for the origin is plotted for several values of delay in Fig. 2.

Because the stability region closes in the negative half-plane for  $\tau > 0$ , it is possible for the origin to lose stability due to large *negative* connection eigenvalues—even purely real ones. The intersection of the stability region border and the  $\text{Re}(\lambda)$  axis in the negative half-plane is given by the solution to Eq. (3.10a) at  $\theta = \pi$ . We define this solution as  $\Lambda$ , dropping the argument for the special case  $\theta = \pi$ . The value of  $\Lambda$  is inversely proportional to the gain of the neurons and is a transcendental function of delay defined implicitly by Eq. (3.10). A plot of the product  $\Lambda\beta$ , which depends only on delay, is shown in Fig. 3. For large and small delay,  $\Lambda$  can be approximated as an explicit function of delay and gain:

$$\Lambda \cong \begin{cases} (1/\beta)(\pi/2\tau), & \tau \ll 1 \\ (1/\beta)\{1 + [\pi/(\tau+1)]^2\}^{1/2}, & \tau \gg 1. \end{cases} \quad (3.11a)$$

$$\Lambda \cong \begin{cases} (1/\beta)(\pi/2\tau), & \tau \ll 1 \\ (1/\beta)\{1 + [\pi/(\tau+1)]^2\}^{1/2}, & \tau \gg 1. \end{cases} \quad (3.11b)$$

For a symmetric connection matrix ( $\lambda_i$  real) the origin

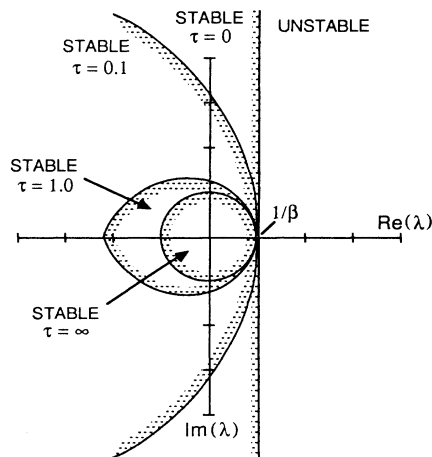


FIG. 2. The stability of the origin in the delay network lies within a closed region in the complex plane of eigenvalues of the connection matrix  $J_{ij}$ . Regions of stability are plotted for different values of delay: For  $\tau = 0$ , the border is a horizontal line at  $\text{Re}(\lambda) = 1/\beta$  as in Fig. 1. For  $\tau = \infty$ , the stability region is a circle of radius  $1/\beta$  centered at the origin of the  $\lambda$  plane. At finite delay, the stability region is teardrop shaped, crossing the real axis in the positive half-plane at  $1/\beta$  and crossing the real axis in the negative half-plane at a delay-dependent value  $\Lambda$ . The tick marks along both axes are in units of  $1/\beta$ .

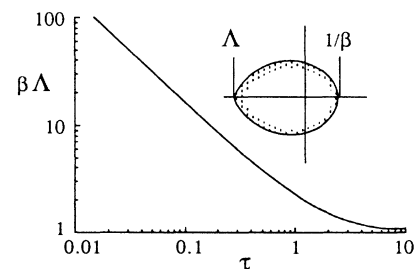


FIG. 3. The border of the stability region crosses the  $\text{Re}(\lambda)$  axis in the negative half-plane at  $\Lambda$  for  $\tau > 0$ . The product  $\Lambda\beta$ , where  $\beta$  is the neuron gain, is plotted as a function of normalized delay  $\tau$ . The value of  $\Lambda$  is particularly important for symmetric networks where the eigenvalues are confined to the  $\text{Re}(\lambda)$  axis.

will be unstable when  $\lambda_{\max} > 1/\beta$  or  $\lambda_{\min} < -\Lambda$ . The bifurcation at  $\lambda_{\max} = 1/\beta$  is a pitchfork (as it is for  $\tau=0$ ) corresponding to a single real root  $s_i$  of Eq. (3.3) passing into the half-plane  $\text{Re}(s_i) > 0$ . The bifurcation at  $\lambda_{\min} = -\Lambda$  corresponds to a Hopf bifurcation<sup>19</sup> of the origin, with a complex pair of roots  $s_i$  passing into the half-plane  $\text{Re}(s) > 0$  at  $\pm\omega_i$ . The imaginary component  $\omega_i = (\beta\Lambda - 1)^{1/2}$  at the bifurcation gives the approximate frequency of the oscillatory mode that results from this bifurcation.

#### D. Symmetric networks with delay

Figure 4 shows the evolution of the stability region of the origin for a delay network at three different values of gain. Each frame also shows schematically a distribution of eigenvalues for one of two types of symmetric networks: The eigenvalues on the left side of Fig. 4 are skewed negative, that is  $|\lambda_{\max}/\lambda_{\min}| < 1$ , while the eigenvalue on the right side are skewed positive, with  $|\lambda_{\max}/\lambda_{\min}| > 1$ . At low gain [Figs. 4(a) and 4(b)] all eigenvalues lie within the large stability region, and the ori-

gin is the unique fixed point and is stable. As the gain is increased, the size of the stability region decreases as  $1/\beta$ . The first eigenvalue to leave the stability region will either be the most negative  $\lambda_{\min}$ , as in Fig. 4(c), or the most positive  $\lambda_{\max}$ , as in Fig. 4(d). For the case in Fig. 4(d), a pair of attracting fixed points appear on either side of the origin along the eigenvector associated with  $\lambda_{\max}$ , and the origin becomes a saddle. For the case in Fig. 4(c), an oscillatory attractor exists along the eigenvector associated with the eigenvalue  $\lambda_{\min}$ . The value of gain at which  $\lambda_{\min}$  leaves the stability region in Fig. 4(c) is given by

$$\beta = -\frac{(\omega^2 + 1)^{1/2}}{\lambda_{\min}}, \quad \omega = -\tan(\omega\tau) \quad \left( \frac{\pi}{2} < \omega\tau < \pi \right). \quad (3.12)$$

In the limit of small delay, this value of gain is

$$\beta \cong -\frac{\pi}{2\tau\lambda_{\min}} \quad (\tau \ll 1). \quad (3.13)$$

The period of oscillation is approximately  $2\pi/\omega$  ( $\cong 4\tau$  for  $\tau \ll 1$ ).

For an eigenvalue distribution which satisfies  $|\lambda_{\max}/\lambda_{\min}| < 1$ , the first bifurcation to occur as the gain is increased can be either a pitchfork bifurcation as  $\lambda_{\max}$  leaves the stability region, or a Hopf bifurcation as  $\lambda_{\min}$  leaves the stability region, depending on the value of delay. For an eigenvalue distribution which satisfies  $|\lambda_{\max}/\lambda_{\min}| > 1$ ,  $\lambda_{\max}$  will always leave the stability region before  $\lambda_{\min}$  regardless of delay.

A stability criterion for symmetric networks based on linear stability analysis can be formulated by requiring that  $\lambda_{\min}$ , the minimum eigenvalue of  $J_{ij}$ , remain inside of the negative border of the stability region of the origin. In terms of the notation we have defined, this criterion requires  $-\Lambda < \lambda_{\min}$ . The condition can be simplified by noting that  $\Lambda$  is always larger than its small-delay limit of  $\pi/(2\tau\beta)$ . The stability criterion for symmetric networks with delay can thus be stated

$$\tau < -\frac{\pi}{2\beta\lambda_{\min}} \implies \text{no sustained oscillation}. \quad (3.14)$$

This criterion lacks the rigor of a global stability condition, which exists for  $\tau=0$ ,<sup>4,5</sup> but is supported by considerable numerical and experimental evidence.

Figures 4(e) and 4(f) show the situation when the gain is sufficiently large that eigenvalues have left the stability region through both negative and positive borders, indicating that Eq. (3.14) is violated and that fixed points away from the origin exist. In this regime the system possesses multiple basins of attraction for coexisting fixed-point and oscillatory attractors.

We find experimentally and numerically that delay networks may or may not show sustained oscillation in this large-gain regime, depending on the value of delay and the eigenvalue distribution. The observed behavior at large gain may be classified according to the ratio  $|\lambda_{\max}/\lambda_{\min}|$ : Networks with  $|\lambda_{\max}/\lambda_{\min}| > 1$ , as in Fig.

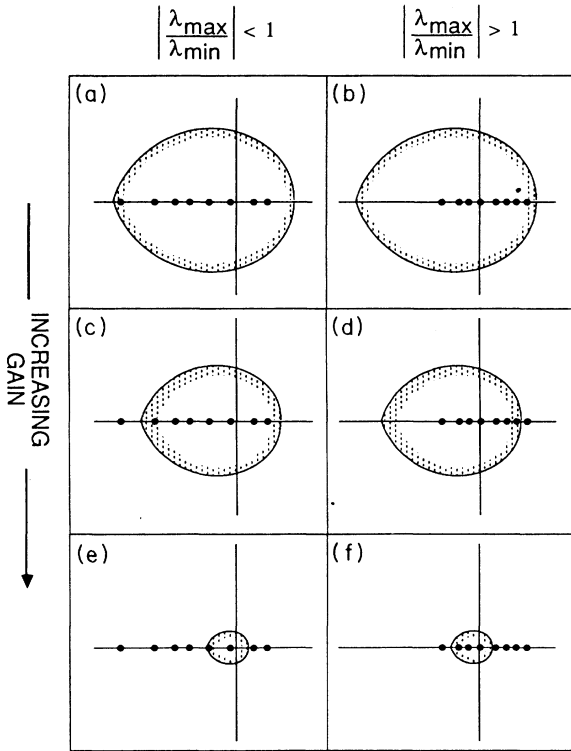


FIG. 4. The stability region of the origin and two different types of eigenvalue distributions (solid circles) are shown schematically. On the left (a,c,e), the eigenvalues satisfy  $|\lambda_{\max}/\lambda_{\min}| < 1$ ; on the right (b,d,f), the eigenvalues satisfy  $|\lambda_{\max}/\lambda_{\min}| > 1$ . As the gain is increased, the stability region decreases in size, and the origin loses stability. The bifurcations for each type of distribution are explained in the text.

4(f), either do not oscillate at all or will oscillate only when the delay is much larger than the relaxation time. We have never observed sustained oscillation at  $\tau < 1$  in any network satisfying  $|\lambda_{\max}/\lambda_{\min}| > 1$  experimentally or numerically. We do not stress the distinction between networks which do not oscillate at *any* delay and those which only oscillate at very long delay. While this distinction is interesting and especially important for parallel-update networks, which corresponds to the  $\tau \rightarrow \infty$  limit of our network, as a design criterion for continuous-time networks with small delay, the claim that delay networks with  $|\lambda_{\max}/\lambda_{\min}| > 1$  do not oscillate except perhaps at very large delay is the result of interest. This result remains empirical, but we show in Sec. IV that it is consistent with an analytical result for networks which oscillate coherently.

In contrast, all networks investigated satisfying  $|\lambda_{\max}/\lambda_{\min}| < 1$  will oscillate for sufficient delay. At large gain, as in Fig. 4(e), these networks show coexisting fixed-point and oscillatory attractors. The basins of attraction for the oscillatory attractors are large for large delay but shrink as the delay is decreased.<sup>18</sup> For delay less than a critical value  $\tau_{\text{crit}}$ , the oscillatory attractors disappear, and only fixed-point dynamics are observed. A value for  $\tau_{\text{crit}}$  cannot be found by the linear stability analysis described in this section because of the importance of the nonlinearity in the large-gain regime. An expression for  $\tau_{\text{crit}}$  for networks which oscillate coherently (defined below) is derived in Sec. IV. The critical delay  $\tau_{\text{crit}}$  found in this case diverges as  $|\lambda_{\max}/\lambda_{\min}| \rightarrow 1$ , in agreement with the empirical results above.

#### E. Self-connection in delay networks

For the networks described in this paper the diagonal elements of the connection matrix have been set to zero, indicating that there is no feedback from a neuron directly to itself. This convention is not necessary for stability when the network dynamics are in continuous time.<sup>26</sup> Including a delayed self-connection affects the dynamics by shifting the eigenvalue distribution and by decreasing the relaxation time of the network.

We consider as an example the effect of adding a delayed self-connection term to the all-inhibitory network. The normalized connection matrix and eigenvalues when a self-connection  $\delta$  (assumed real) is included are given by

$$J_{ij} = \frac{1}{N-1+|\delta|} \begin{pmatrix} \delta & -1 & -1 & \cdots & -1 \\ -1 & \delta & -1 & & -1 \\ -1 & -1 & \delta & & -1 \\ \cdots & & & \cdots & \cdots \\ -1 & -1 & -1 & \cdots & \delta \end{pmatrix}, \quad (3.15a)$$

$$\lambda_i = \begin{cases} \frac{1+\delta}{N-1+|\delta|} & (N-1 \text{ degenerate}) \\ \frac{(1-N)+\delta}{N-1+|\delta|} & (\text{once}). \end{cases} \quad (3.15b)$$

The connection eigenvalues  $\lambda_{\max}$  and  $\lambda_{\min}$  for the all-inhibitory network are shown as a function of self-connection  $\delta$  in Fig. 5. Notice that adding a negative

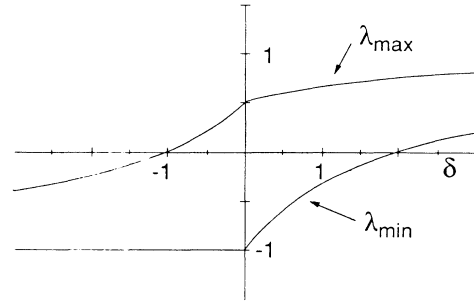


FIG. 5. The largest and smallest eigenvalues (solid lines) for the all-inhibitory network, Eq. (3.15), plotted as a function of the diagonal element  $\delta$ . The values indicated at the axis crossings are for a general  $N$ , but the scale of the drawing is correct for the case  $N=3$ . The asymptotic value for all eigenvalues as  $\delta \rightarrow \pm \infty$  is  $\pm 1$ .

self-connection ( $\delta < 0$ ) does not change  $\lambda_{\min}$ , thus the value of delay where the Hopf bifurcation occurs in the all-inhibitory network is not changed by a negative self-connection. Adding a positive self-connection ( $\delta > 0$ ) will bring  $\lambda_{\min}$  closer to zero and will increase the delay necessary for the Hopf bifurcation to occur. The condition  $|\lambda_{\max}/\lambda_{\min}| > 1$  is satisfied in (3.15) when the self-connection  $\delta$  exceeds  $(N/2 - 1)$ .

#### IV. CRITICAL DELAY IN THE LARGE-GAIN LIMIT

In this section we find a critical delay for sustained oscillation in the large-gain regime, where fixed-point attractors away from the origin coexist with a single coherent oscillatory attractor. The main result, Eq. (4.4), applies to networks in which the oscillatory attractor is along a coherent direction. Coherence is defined by the condition that all  $|u_i|$  are equal. Equivalently, a coherent oscillatory attractor lies along a vector pointing to any corner of an  $N$ -dimensional hypercube centered at the origin. When the eigenvector associated with  $\lambda_{\min}$  is in a coherent direction, then the most robust oscillatory mode—that is, the one that will exist at the smallest delay—will be coherent. In this case, the network will not oscillate when the delay is smaller than the critical delay derived below. Connection topologies which have a coherent direction associated with  $\lambda_{\min}$  include fully frustrated networks (the all-inhibitory network and all Mattis transformations<sup>24</sup>) and symmetrically connected frustrated rings. For other networks discussed in Sec. V, including the diluted inhibitory network and the negative-only clipped Hebb rule, the eigenvector associated with  $\lambda_{\min}$  appears numerically to approach coherence at large  $N$ , though this has not been proven rigorously.

The stability criterion of Sec. III, Eq. (3.14), based on linear stability analysis, applies at all values of gain but becomes useless in the large-gain limit. In particular, Eq. (3.14) requires that the delay vanish as the gain diverges in order to prevent oscillation. In contrast, we find experimentally and numerically that as the gain becomes large the critical delay below which oscillation vanishes

approaches a gain-independent limit. We believe that this gain-independent critical delay results from an instability of the oscillatory attractor itself. Below, we derive a value for the critical delay  $\tau_{\text{crit}}$  for sustained coherent oscillation in the large-gain limit by considering the stability of the oscillatory attractor. For  $\tau < \tau_{\text{crit}}$  sustained oscillation should vanish. As shown below, this novel stability criterion agrees very well with experimental and numerical data.

#### A. Effective gain along the coherent oscillatory attractor

The basic idea of the derivation is that neurons with saturating output can be regarded as having an “effective gain”  $\beta_{\text{eff}}$  that is not constant along the oscillatory attractor and can be finite even when  $f(u)$  is infinitely steep at  $u=0$ . The effective gain is defined as  $\beta_{\text{eff}} = f(u(t))/u(t)$ . Note that  $\beta_{\text{eff}}$  is defined as the ratio of neuron output  $f(u(t))$  divided by the input  $u(t)$  which produced that output; for a delay network,  $f(u(t))$  does not appear at the output until a time  $\tau$  after  $u(t)$  appears at the input. This definition of  $\beta_{\text{eff}}$  reduces to the usual gain  $\beta$  when  $f(u)$  is linear (with or without delay). We assume that the oscillatory attractor loses stability when the variable effective gain is sufficiently large at all points on the attractor that perpendicular perturbations will always lead the system off of the attractor. This instability occurs when the minimum value of  $\beta_{\text{eff}}$  along the attractor exceeds a critical value related to flow perpendicular to the oscillation direction.

When the large-gain network is oscillating coherently, neuron outputs swing between  $\pm 1$  in the form of a square wave, while the inputs alternately charge and discharge exponentially with a time constant equal to the relaxation time of the network as shown in Fig. 6(a). The smallest value of  $\beta_{\text{eff}}$  occurs when the input amplitude is at the maximum of its charge-discharge oscillation and the corresponding output is saturated at  $\pm 1$ . At this point,  $\beta_{\text{eff}}$  is the reciprocal of this input amplitude. The maximum amplitude  $A_i$  at the  $i$ th input depends on the delay and is given by

$$A_i = \left| \sum_j J_{ij} \text{sgn}(u_j) \right| (1 - e^{-\tau}). \quad (4.1)$$

For coherent oscillation along the direction associated with  $\lambda_{\text{min}}$  all of the  $A_i$  in Eq. (4.1) will be the same (defined as  $A$ ) and the term in absolute value brackets will be equal to  $-\lambda_{\text{min}}$  ( $> 0$ ). In this case  $\beta_{\text{eff}}$  will be bounded below by  $1/A$ , as shown in Fig. 6(c):

$$\beta_{\text{eff}} \geq \frac{1}{A} = -\frac{1}{\lambda_{\text{min}}(1 - e^{-\tau})}. \quad (4.2)$$

Flow perpendicular to the oscillatory attractor is described by Eq. (3.2) with  $\lambda_i$  equal to the  $N-1$  eigenvalues of  $J_{ij}$  excluding  $\lambda_{\text{min}}$  and with  $\beta = \beta_{\text{eff}}$ . The least stable of the  $N-1$  directions perpendicular to the oscillatory attractor is along the eigenvector associated with  $\lambda_{\text{max}}$ . Thus the attractor will lose stability when  $\lambda_{\text{max}}\beta_{\text{eff}} > 1$  all along the oscillatory trajectory. From Eq. (4.2), this condition is satisfied when  $\lambda_{\text{max}}/A > 1$ . The critical delay

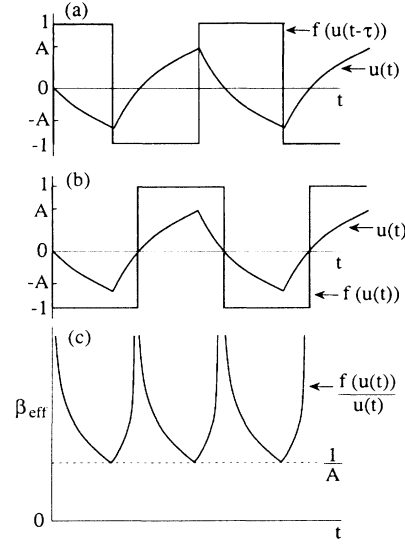


FIG. 6. (a) The input  $f(u(t))$  (triangular wave) and output  $f(u(t-\tau))$  (square wave) for a saturating infinite-gain neuron with delay in an oscillatory state. The value  $A$ , given by Eq. (4.1), is the maximum amplitude of the input. (b) The same input and output waveforms as above with the offset between input and output due to delay suppressed. (c) The effective gain  $\beta_{\text{eff}}$ , defined as the ratio of  $f(u(t))/u(t)$ , takes on finite values even when  $f(u)$  is infinitely steep at  $u=0$ . The minimum value of  $\beta_{\text{eff}}$  is where the input is maximum; at this point  $\beta_{\text{eff}} = 1/A$ .

$\tau_{\text{crit}}$ , defined by the condition  $\lambda_{\text{max}}/A = 1$ , is thus given by

$$\lambda_{\text{max}} \left( \frac{1}{-\lambda_{\text{min}}(1 - e^{-\tau_{\text{crit}}})} \right) = 1. \quad (4.3)$$

Solving for  $\tau_{\text{crit}}$  gives the main result of Sec. IV,

$$\tau_{\text{crit}} = -\ln \left[ 1 + \frac{\lambda_{\text{max}}}{\lambda_{\text{min}}} \right] \quad (0 < \lambda_{\text{max}} < -\lambda_{\text{min}}). \quad (4.4)$$

To illustrate this result we again consider the  $N \times N$  all-inhibitory network Eq. (3.6) in the large-gain limit. This network has connection eigenvalues  $\lambda_{\text{max}} = 1/(N-1)$ ,  $\lambda_{\text{min}} = -1$ , giving a large-gain critical delay

$$\tau_{\text{crit}} = \ln \left[ \frac{N-1}{N-2} \right] \left[ \sim \frac{1}{N} \text{ for large } N \right]. \quad (4.5)$$

Figure 7 shows  $\tau_{\text{crit}}$  for the all-inhibitory networks as a function of the size of the network  $N$ . The solid line is from Eq. (4.5); the circles are data from numerical integration with  $\beta = 40$  indicating the smallest delay that would support sustained oscillation. The rapid decrease in  $\tau_{\text{crit}}$  as the size of the network increases indicates that the all-inhibitory network is very prone to oscillation for large  $N$ .

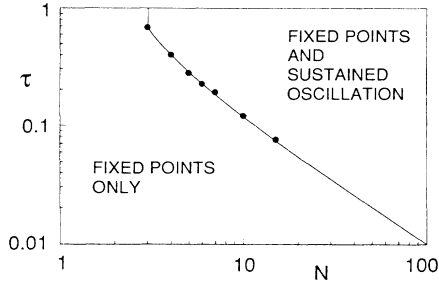


FIG. 7. Large-gain critical delay  $\tau_{\text{crit}}$  for the all-inhibitory network plotted against  $N$ , the size of the network. The solid line is the theory from Eq. (4.4), the filled circles are from numerical integration of the delay equations at  $\beta=40$ . Numerical integration data were obtained by starting the system with initial functions  $\phi_i: [-\tau, 0]$  along the eigenvector associated with  $\lambda_{\text{min}}$  and constant over the interval  $[-\tau, 0]$ . The delay equations were integrated with Euler method integration and checked for oscillation after many (up to  $10^4$ ) time constants. The critical delay was found by repeating the integration using a ten-split binary search in the value of delay.

### B. Crossover from low-gain to high-gain regime

We have now found two critical values of delay: For small gain ( $\beta < \lambda_{\text{max}}$ ) the network does not oscillate for  $\tau < \tau_H$ , where  $\tau_H$  is the value of delay where the Hopf bifurcation occurs. For small delay,

$$\tau_H \cong -\frac{\pi}{2\beta\lambda_{\text{min}}}. \quad (4.6)$$

At large gain, the delay network does not oscillate for  $\tau < \tau_{\text{crit}}$ , where  $\tau_{\text{crit}}$  is given by Eq. (4.4). We now consider the crossover from the small-gain regime to the large-gain regime for the specific example of a mutually inhibitory triangle of neurons. For this network,

$$J_{ij} = \frac{1}{2} \begin{pmatrix} 0 & -1 & -1 \\ -1 & 0 & -1 \\ -1 & -1 & 0 \end{pmatrix}, \quad \lambda_{\text{max}} = \frac{1}{2}, \quad \lambda_{\text{min}} = -1. \quad (4.7)$$

Figure 8(a) shows the two theoretical curves for each of the two regimes. The data points are the values of delay where the oscillatory attractor disappears as measured in the analog circuit (open circles) and by numerically integrating the delay equations (filled circles). Figure 8(b) describes the four regions of the  $\beta$ - $\tau$  plane with distinct dynamics. For  $\beta < 2$  and  $\tau < \tau_H$ , where  $\tau_H$  is found by setting  $\lambda_{\text{min}} = -1$  in Eq. (3.12), there is a single fixed-point attractor at the origin. For  $\beta < 2$ ,  $\tau > \tau_H$ , the fixed point at the origin is unstable, and there is a single oscillatory attractor. At  $\beta = 2$  a fixed point away from the origin appears. At this crossover point,  $\tau_H \cong 1.209$ . For  $\beta > 2$ , the Hopf bifurcation line no longer marks the critical delay for sustained oscillation. As  $\beta$  becomes large, the critical delay for sustained oscillation approaches the gain-independent theoretical value of  $\tau_{\text{crit}}$ . From Eq. (4.5),  $\tau_{\text{crit}}(N=3) = \ln 2 \cong 0.693$ .

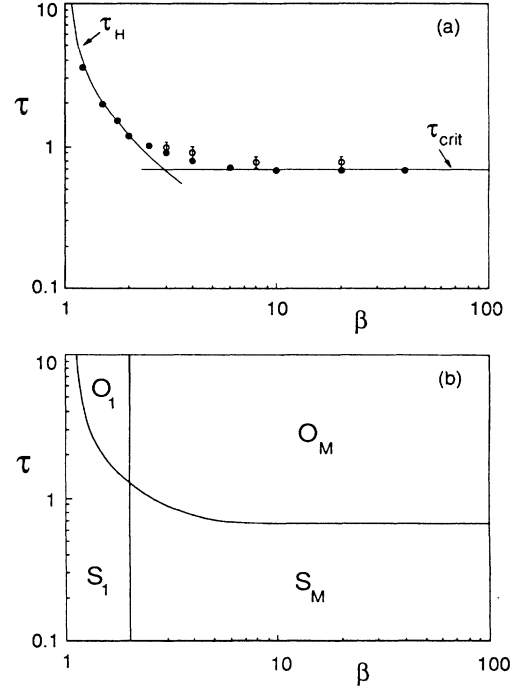


FIG. 8. Phase diagram for the all-inhibitory (or frustrated) triangle of delay neurons. (a) Two theoretical curves are shown as solid lines: The line labeled  $\tau_H$  indicates the value of delay and gain where the origin undergoes a Hopf bifurcation, from Eq. (3.14); the line labeled  $\tau_{\text{crit}}$  indicates the large-gain critical delay where the oscillatory mode loses stability. Below  $\tau_{\text{crit}}$  only fixed-point attractors are stable. The data points are critical delays measured in the electronic network (open circles) and by numerical integration (solid circles) with  $\beta=40$ . Numerical integration data were obtained as described in the caption of Fig. 7. (b) The four regions in the  $\beta$ - $\tau$  plane with qualitatively different dynamics are  $S_1$ , single fixed-point attractor at the origin;  $O_1$ , single coherent oscillatory attractor;  $S_M$ , multiple fixed-point attractors away from the origin;  $O_M$ , multiple attractors away from the origin, including fixed points and a coherent oscillatory attractor.

## V. STABILITY OF PARTICULAR NETWORK CONFIGURATIONS

In this section we consider sustained oscillation in three symmetric delay networks: (1) symmetrically connected inhibitory rings; (2) randomly connected symmetric networks; and (3) Hebb rule and clipped Hebb rule associative memories.

### A. Symmetrically connected rings

A ring of neurons with symmetric connections all of equal strength but of either sign, inhibitory or excitatory, has a spectrum of connection eigenvalues given by

$$\lambda_k = \cos[(2\pi/N)(k + \varphi)], \quad k = 0, 1, 2, \dots, (N-1), \quad (5.1)$$

where  $\varphi = \frac{1}{2}$  for a frustrated ring, i.e.,

$$\text{sgn} \left[ \prod_{\text{ring}} J_{ij} \right] = -1,$$

and  $\varphi = 0$  for a nonfrustrated ring.<sup>27</sup> The ratio of maximum to minimum eigenvalues can be found directly from Eq. (5.1):

$$\left| \frac{\lambda_{\max}}{\lambda_{\min}} \right| = \begin{cases} \cos \left[ \frac{\pi}{N} \right] & (< 1), \quad N \text{ odd; frustrated} \\ 1, & N \text{ even} \\ \sec \left[ \frac{\pi}{N} \right] & (> 1), \quad N \text{ odd; nonfrustrated.} \end{cases} \quad (5.2)$$

Only frustrated rings with odd  $N$  satisfy  $|\lambda_{\max}/\lambda_{\min}| < 1$ , suggesting that only these configurations will show sustained oscillation. This is confirmed experimentally and numerically. In the large-gain limit, the critical delay  $\tau_{\text{crit}}$  is found from Eq. (4.4), giving

$$\tau_{\text{crit}} = -\ln[1 - \cos(\pi/N)] \quad (N \text{ odd; frustrated}). \quad (5.3)$$

Notice that  $\tau_{\text{crit}}$  increases with increasing  $N$  for the symmetric ring while for the all-inhibitory network  $\tau_{\text{crit}}$  decreases as  $1/N$ . Inhibitory rings are thus much less prone to oscillation than fully connected inhibitory networks. The critical delays from numerical integration are compared to Eq. (5.3) in Fig. 9.

### B. Random symmetric networks

Oscillations in randomly connected neural networks have been considered previously for symmetric random networks with parallel-update dynamics, which show at most period-2 oscillations<sup>14-17</sup> and for asymmetric net-

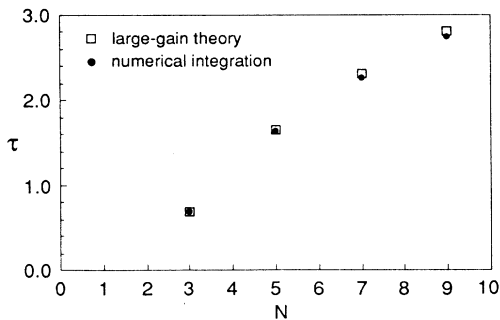


FIG. 9. Large-gain critical delay  $\tau_{\text{crit}}$  for symmetrically connected frustrated rings with  $N=3,5,7,9$  from Eq. (5.3) (open squares) is plotted along with critical delay from numerical integration (filled circles) with  $\beta=40$ . Numerical integration data were obtained as described in the caption of Fig. 7. Frustrated symmetric rings with even  $N$  do not satisfy  $|\lambda_{\max}/\lambda_{\min}| < 1$  and therefore are not expected to oscillate for any delay within the large-gain theory. Numerically, frustrated rings with even  $N$  showed sustained oscillation only for very large delay ( $\tau > 10$ ), though this is possibly a numerical artifact.

works with parallel-update dynamics,<sup>28-31</sup> Monte Carlo dynamics,<sup>29,30</sup> and continuous-time dynamics.<sup>32-34</sup> Asymmetric random networks are capable of a wider range of dynamics than symmetric random networks, including chaos.<sup>33,34</sup> Periodic and chaotic dynamics in a symmetric mean-field magnetic model with delayed interaction have also been described.<sup>35</sup>

We only consider the effect of delay in symmetric networks, and find only simple (nonchaotic) oscillation above a critical delay. The absence of chaos in the symmetric continuous-time delay network (with monotonic nonlinearity) is not surprising, as the two limits of short and long delay are known to possess only fixed points and period-2 oscillations. Rigorous proof of this conjecture has not been presented to our knowledge.

We consider delay networks with symmetric connection matrices whose elements  $J_{ij}$  ( $=J_{ji}$ ) are independently fixed at one of three values ( $+, -, 0$ ). Any two neurons are connected by a positive connection with probability  $p_+$  and by a negative connection with probability  $p_-$ . The *connectance*  $p$  is defined as  $p = (p_+ + p_-)$ ; the *bias*  $q$  is defined as  $q = (p_+ - p_-)$ . Using the normalization of  $J_{ij}$  described in Sec. II, the connection matrix is given by

$$J_{ij} = J_{ji} = \begin{cases} \pm 1/pN & \text{with probability } p_{\pm} \\ 0 & \text{with probability } 1-p. \end{cases} \quad (5.4)$$

The eigenvalue spectrum of a random symmetric matrix is described by the Wigner semicircular law.<sup>36-38</sup> The notation used here follows Ref. 37. For an  $N \times N$  random symmetric matrix whose elements have a mean  $M_0/N$  and a variance  $\sigma^2/N$ , the spectrum of eigenvalues  $\rho(\lambda)$  converges for large  $N$  to a continuous distribution, for  $M_0=0$ ,

$$\rho_0(\lambda) = \begin{cases} (4\sigma^2 - \lambda^2)/2\pi\sigma^2, & |\lambda| < 2\sigma \\ 0, & |\lambda| > 2\sigma \end{cases} \quad (5.5a)$$

and for  $M_0 \neq 0$ ,

$$\rho(\lambda) = \begin{cases} \rho_0(\lambda), & |M_0| < \sigma \\ \rho_0(\lambda) + \frac{1}{N} \delta(\lambda - M_0 + (\sigma^2/M_0)), & |M_0| > \sigma. \end{cases} \quad (5.5b)$$

For the  $(+, -, 0)$  matrix [Eq. (5.4)] we identify

$$M_0 \leftrightarrow \frac{q}{p}, \quad (5.6a)$$

$$\sigma^2 \leftrightarrow \frac{1}{p^2 N} (p - q^2). \quad (5.6b)$$

From Eqs. (5.5) and (5.6), we can find the maximum and minimum eigenvalues of  $J_{ij}$ . Setting  $J_{ii}=0$  will add a term of order  $O(1/N)$  to all of the eigenvalues; we will neglect this and all terms  $O(1/N)$ . These results are therefore valid only for large  $N$ , where  $N^{1/2} \ll N$ .

$$\lambda_{\max} = \begin{cases} \frac{2}{p} [(p - q^2)/N]^{1/2} + O(1/N) & \text{for } q < (p/N)^{1/2} \\ \frac{q}{p} + O(1/N) & \text{for } q > (p/N)^{1/2}, \end{cases} \quad (5.7a)$$

$$\lambda_{\min} = \begin{cases} -\frac{2}{p} [(p - q^2)/N]^{1/2} + O(1/N) & \text{for } -q < (p/N)^{1/2} \\ \frac{q}{p} + O(1/N) & \text{for } -q > (p/N)^{1/2}. \end{cases} \quad (5.7b)$$

The condition  $|\lambda_{\max}/\lambda_{\min}| < 1$  is only satisfied when  $-q > (p/N)^{1/2}$ , suggesting that a symmetric random network must be biased sufficiently negative before it will oscillate for small delay.

An example of a random symmetric network that will oscillate for small delay is the randomly diluted inhibitory network. For this network  $p_+ = 0$  and  $p = -q = p_-$ . Ignoring terms of  $O(1/N)$ , the maximum and minimum eigenvalues are

$$\lambda_{\max} = \frac{2}{\sqrt{N}} \left[ \frac{1}{p_-} - 1 \right]^{1/2}, \quad (5.8a)$$

$$\lambda_{\min} = -1. \quad (5.8b)$$

Figure 10 shows the theoretical range of eigenvalues for a  $100 \times 100$  randomly diluted inhibitory matrix as a function of connectance  $p_-$ . The small crosses are the calculated eigenvalues for a computer generated random  $(-, 0)$  matrix for  $p_- = 0.4, 0.7,$  and  $0.9$ .

For the randomly diluted inhibitory network, with or without delay, the neuron gain at which the origin becomes unstable via a pitchfork bifurcation, creating fixed points away from the origin, is given by

$$\beta = \frac{\sqrt{N}}{2} \left[ \frac{1}{p_-} - 1 \right]^{-1/2} \quad (\text{pitchfork}). \quad (5.9)$$

Because  $\lambda_{\min}$  is independent of connectance the delay at which the origin loses stability by a Hopf bifurcation is also independent of connectance. Inserting  $\lambda_{\min} = -1$  into Eq. (4.6) gives  $\tau_H \cong \pi/2\beta$ , the small-delay limit being appropriate for large  $N$  and therefore large  $\beta$ .

The large-gain analysis of Sec. IV can be applied to the diluted inhibitory network when  $N$  is large. At large  $N$  the eigenvector associated with  $\lambda_{\min}$  is nearly coherent, that is, the differences in  $|u_i|$  along the eigenvector associated with  $\lambda_{\min}$  are small compared to  $|u_i|$  and appear numerically to vanish as  $N \rightarrow \infty$ . Applying Eq. (4.4) gives a gain-independent critical delay which does depend on the connectance. From Eqs. (4.4) and (5.8), the randomly diluted inhibitory network will not oscillate in the large-gain limit for  $\tau < \tau_{\text{crit}}$ , where

$$\tau_{\text{crit}} = -\ln \left[ 1 - \frac{2}{\sqrt{N}} \left[ \frac{1}{p_-} - 1 \right]^{1/2} \right]. \quad (5.10)$$

Figure 11 shows  $\tau_{\text{crit}}$  as a function of connectance  $p_-$  for  $N = 1000$ .<sup>39</sup> This figure shows that for a very mild dilution of connections,  $\tau_{\text{crit}}$  is greatly increased, but addi-

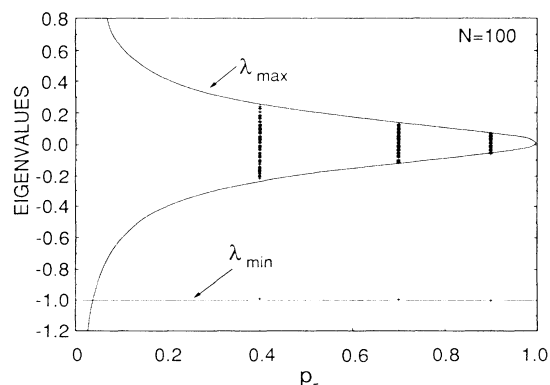


FIG. 10. The range of connection eigenvalues for a symmetrically diluted inhibitory network with  $N = 100$  from Eqs. (5.5) and (5.6) is plotted as a function of the connectance  $p_-$  (solid lines). The horizontal line at  $-1$  indicates a single eigenvalue  $\lambda_{\min}$  lying outside of the quasicontinuous distribution. The small crosses are eigenvalues computed for a randomly generated symmetric  $100 \times 100$  matrix with  $p_- = 0.4, 0.7,$  and  $0.9$ .

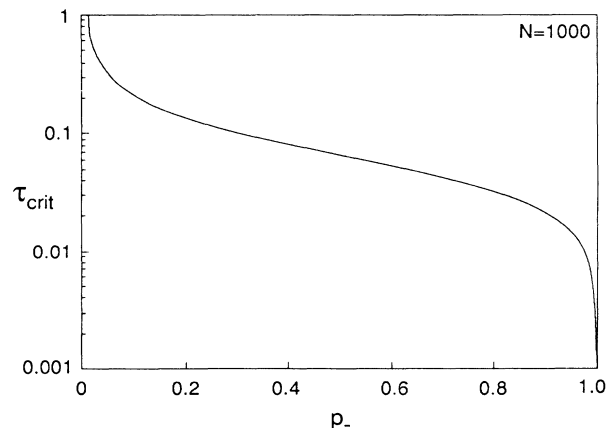


FIG. 11. Plot of the large-gain critical delay  $\tau_{\text{crit}}$  as a function of connectance  $p_-$  for the diluted inhibitory network with  $N = 1000$  (Ref. 39). Note that very mild dilution greatly increases  $\tau_{\text{crit}}$ .

tional dilution does little to further increase  $\tau_{\text{crit}}$ . When the dilution is mild ( $p_- \sim 1$ ), the right-hand side of Eq. (5.10) can be expanded to yield

$$\tau_{\text{crit}} \cong \left( \frac{4d}{N} \right)^{1/2} \left[ \frac{1}{N} \ll d \ll 1 \right], \quad (5.11)$$

where  $d = 1 - p_- (\ll 1)$  is a small random dilution. Equation (5.11) can be compared to the critical delay for the undiluted all-inhibitory network, Eq. (4.5), to give a simple expression for the increase in critical delay due to random dilution

$$\frac{\tau_{\text{crit}}^{(\text{diluted})}}{\tau_{\text{crit}}^{(\text{undiluted})}} \cong \sqrt{4dN} \left[ \frac{1}{N} \ll d \ll 1 \right]. \quad (5.12)$$

This result demonstrates how small random dilution of a large inhibitory network can be used to stabilize a network by increasing the critical delay for sustained oscillation.

### C. Associative memory networks

Associative memory networks are designed to converge to one of many fixed points (“memories”) away from the origin. Which memory is retrieved depends on the initial state of the network. The existence of many attractors each with a basin of attraction is essential to the dynamics of an associative memory.

A variety of algorithms for adjusting the interconnections to efficiently encode memories have been developed.<sup>6</sup> Certainly the most commonly used is the Hebb rule<sup>20</sup> or outer product rule, where the interconnection matrix is of the form

$$J_{ij} = \frac{1}{N} \sum_{\alpha=1}^m \xi_i^{\alpha} \xi_j^{\alpha},$$

$$J_{ii} = 0, \quad \xi_i = \{\text{random string of } \pm 1\text{'s}\}, \quad (5.13)$$

where  $m$  is the number of memories stored. For  $m \ll N$ , the eigenvalue distribution for a Hebb rule matrix with  $m$  random memories has  $m$  large positive elements of magnitude  $\sim 1$ , and  $(N - m)$  small negative eigenvalues of magnitude  $\sim -m/N$ . Thus the Hebb rule matrix satisfies  $|\lambda_{\text{max}}/\lambda_{\text{min}}| > 1$ , suggesting that it will not oscillate, except perhaps when  $\tau \gg 1$ . Numerically, we find that even very long delays ( $\tau \gg 1$ ) will not induce sustained oscillation in a Hebb rule network. This observation is supported by the recent claim that Hebb rule networks with parallel-update dynamics and two-state (“Ising”) neurons, corresponding to the infinite-gain and infinite-delay limit of our analog delay system, also do not oscillate.<sup>40</sup>

A variation of the Hebb rule that is important for hardware implementation is the clipped Hebb rule, which restricts the interconnection matrix to a few values. The distribution of eigenvalues for a clipped Hebb matrix  $J'_{ij}$  is greatly affected by the details of the clipping algorithm as illustrated in Fig. 12. Figure 12(a) shows the distinct eigenvalues  $\lambda(J'_{ij})$  for the clipping algorithm  $J'_{ij} = (1/Z) \text{sgn}(J_{ij})$ , where  $Z$  is the normalization  $Z = \sum_i |\text{sgn}(J_{ij})|$ . This clipping algorithm introduces

large negative eigenvalues but satisfies  $|\lambda_{\text{max}}/\lambda_{\text{min}}| > 1$  for all  $m$ , suggesting that these networks will not oscillate when the delay is smaller than the network relaxation time. Experimentally and numerically, we find that this clipping algorithm does not produce sustained oscillation until the delay is much longer than the relaxation time. Figure 12(b) shows the distinct eigenvalues for the two-value clipping algorithm  $-J'_{ij} = (1/Z) \Theta(-J_{ij})$ , where  $\Theta$  is the heavyside function and  $Z = \sum_i \Theta(-J_{ij})$ . This clipping algorithm, which sets all positive elements of the unclipped matrix  $J_{ij}$  to 0 and all negative elements to  $-1/Z$ , has the hardware advantage of only requiring a single inverting output from each neuron, as pointed out by Denker,<sup>41</sup> but as seen in Fig. 12(b) introduces a large negative eigenvalue which can lead to sustained oscillation for a neuron delay of the order of the relaxation time ( $\tau \sim 1$ ).

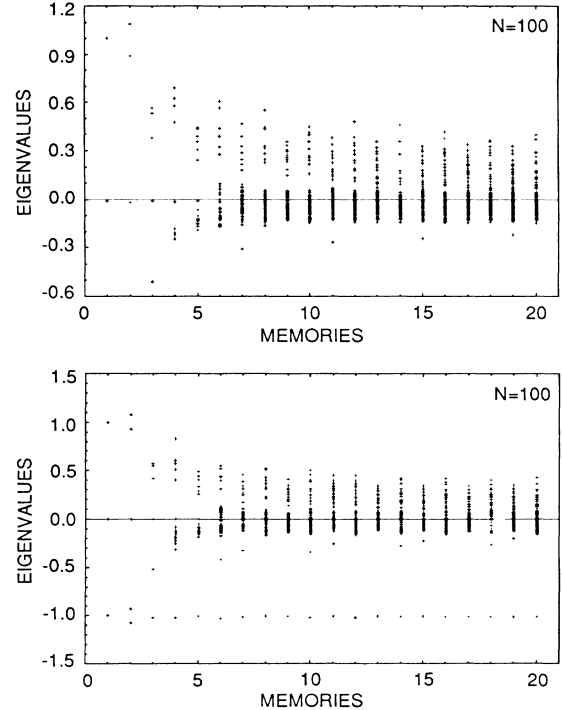


FIG. 12. Connection eigenvalues for clipped Hebb matrices plotted as a function of the number of stored random memories using two clipping algorithms discussed in the text. (a) Hebb matrix  $J_{ij}$  clipped according to  $J'_{ij} = (1/Z) \text{sgn}(J_{ij})$ , with normalization  $Z = \sum_i |\text{sgn}(J_{ij})|$ , gives an unbiased matrix and an eigenvalue distribution which satisfies  $|\lambda_{\text{max}}/\lambda_{\text{min}}| > 1$  for all numbers of memories. (b) Clipping algorithm which sets all positive  $J_{ij}$  to zero and all negative  $J_{ij}$  to  $-1/Z$ , with normalization  $Z = \sum_i \Theta(-J_{ij})$ , has the advantage of only requiring a single output from each neuron, but produces large negative eigenvalues that can lead to sustained oscillation. The data were obtained numerically for a  $100 \times 100$  Hebb matrix  $J_{ij}$  with random memories as in Eq. (5.13).

## VI. DISCUSSION AND REVIEW OF USEFUL RESULTS

In summary, we have considered the stability of analog neural networks with delayed response. The aim has been to extend the stability condition "symmetric connection implies no oscillation," which is valid when the neurons have instantaneous response, to a more realistic model of neural networks where time delay is included. We find that symmetrically connected networks can undergo sustained oscillation when the neurons have delayed output, but only when the ratio of delay to relaxation time exceeds a critical value.

At low neuron gain, linear stability analysis about the origin suggests that for  $\tau < -\pi/(2\beta\lambda_{\min})$  a symmetric network will not oscillate. In this inequality,  $\tau$  is the neuron delay in units of the network relaxation time,  $\beta$  is the gain of the neurons at the origin, and  $\lambda_{\min}$  is the minimum eigenvalue of the connection matrix  $J_{ij}$  in Eq. (2.3).

This stability criterion based on linear stability analysis is valid at all values of gain but becomes uselessly conservative in the large-gain limit. At large neuron gain, fixed points exist away from the origin, and the dynamics are no longer well characterized by linear stability analysis near the origin. Symmetric networks in which the maximum and minimum eigenvalues of the connection matrix satisfy  $|\lambda_{\max}/\lambda_{\min}| > 1$  are not found to oscillate as long as the delay is comparable to or less than the network relaxation time. Symmetric networks with  $|\lambda_{\max}/\lambda_{\min}| < 1$  show coexisting fixed-point and oscillatory attractors at large gain. There exists a critical delay  $\tau_{\text{crit}}$  in the large-gain limit below which oscillatory attractors vanish and only fixed points are found. For symmetric networks in which the oscillatory mode present for the smallest delay is coherent (as defined in Sec. IV), we find sustained oscillation vanishes for  $\tau < \tau_{\text{crit}}$  where  $\tau_{\text{crit}} = -\ln(1 + \lambda_{\max}/\lambda_{\min})$ . This result is independent of gain and is useful as  $\beta \rightarrow \infty$ , unlike the above result based

on linear stability of the origin [Eq. (3.14)].

The stability criteria have been compared to experiments carried out on a small (eight neurons) electronic neural network with controllable time delay and to direct numerical integration of the delay equations with good agreement. Some results for particular network topologies are the following.

(a) The all-inhibitory network is the most oscillation-prone configuration of the delay network. For this configuration, the critical delay in the large-gain limit is given by  $\tau_{\text{crit}} = \ln[(N-1)/(N-2)] \sim 1/N$ , where  $N$  is the size of the network. Thus at large  $N$ , a delay much smaller than the network relaxation time will produce sustained oscillation. Diluting the all-inhibitory network by randomly setting a small fraction  $d \ll 1$  of the interconnections ( $J_{ij}$  and  $J_{ji}$ ) to zero, will increase the critical delay by a factor of  $(4dN)^{1/2}$ .

(b) Rings of symmetrically connected delay neurons will oscillate only when the ring is frustrated

$$\left[ \text{sgn} \left( \prod_{\text{ring}} J_{ij} \right) = -1 \right],$$

and there is an odd number of neurons in the ring.

(c) The Hebb rule matrix, given by Eq. (5.13), satisfies  $|\lambda_{\max}/\lambda_{\min}| > 1$  and is found by numerical integration not to oscillate for arbitrarily long delay. Clipping algorithms, which limit the interconnections to a few strengths, can introduce large negative connection eigenvalues and produce sustained oscillation in networks where the delay is smaller than the network relaxation time.

## ACKNOWLEDGMENTS

We thank S. H. Strogatz for valuable discussions. One of us (C.M.M.) acknowledges financial support from AT&T Bell Laboratories. This research was supported by Joint Services Electronics Program Contract No. N00014-84-K-0465.

<sup>1</sup>Neural Networks for Computing (Snowbird, UT, 1986), Proceedings of the Conference on Neural Networks for Computing, AIP Conf. Proc. 151, edited by J. S. Denker (AIP, New York, 1986).

<sup>2</sup>W. A. Little, Math. Biosci. **19**, 101 (1974); W. A. Little and G. L. Shaw, *ibid.* **39**, 281 (1978).

<sup>3</sup>J. J. Hopfield, Proc. Natl. Acad. Sci. U.S.A. **79**, 2554 (1982).

<sup>4</sup>J. J. Hopfield, Proc. Natl. Acad. Sci. U.S.A. **81**, 3008 (1984).

<sup>5</sup>M. A. Cohen and S. Grossberg, IEEE Trans. SMC-13, 815 (1983).

<sup>6</sup>J. S. Denker, Physica **22D**, 216 (1986).

<sup>7</sup>Proceedings of the Heidelberg Colloquium on Glassy Dynamics, Vol. 275 of Lecture Notes in Physics, edited by J. L. van Hemmen and I. Morgenstern (Springer, Berlin, 1987).

<sup>8</sup>Several articles on hardware implementations of neural networks appear in Appl. Opt. **26**, 4909 (1987).

<sup>9</sup>U. an der Heiden, J. Math. Bio. **8**, 345 (1979).

<sup>10</sup>B. D. Coleman and G. H. Renninger, SIAM J. Appl. Math. **31**, 111 (1976); J. Theor. Bio. **51**, 243 (1975).

<sup>11</sup>K. P. Hadeler and J. Tomiuk, Arch. Rat. Mech. Anal. **65**, 87 (1977).

<sup>12</sup>U. an der Heiden, in Analysis of Neural Networks, Vol. 35 of Lectures Notes in Biomathematics, edited by S. Levin (Springer, New York, 1980).

<sup>13</sup>Application of delay-differential equations to engineering and biology is discussed in V. B. Kolmanovskii and V. R. Nosov, Stability of Functional Differential Equations (Academic, New York, 1986).

<sup>14</sup>P. Peretto, Biol. Cybern. **50**, 51 (1984).

<sup>15</sup>E. Goles-Chacc, F. Fogelman-Soulie, and D. Pellegrin, Disc. Appl. Math. **12**, 261 (1985); E. Goles and G. Y. Vichniac, Ref. 1, p. 165.

<sup>16</sup>G. Grinstein, C. Jayaprakash, and Y. He, Phys. Rev. Lett. **55**, 2527 (1985).

<sup>17</sup>A. Frumkin and E. Moses, Phys. Rev. A **34**, 714 (1986).

<sup>18</sup>C. M. Marcus and R. M. Westervelt, in Neural Information Processing Systems, Denver, CO, 1987, edited by Dana Z. Anderson (AIP, New York, 1988).

<sup>19</sup>Application of the Hopf bifurcation theorem to delay-differential systems is discussed in N. Chaffee, J. Math. Anal. Appl. **35**, 312 (1971).

- Appl. **35**, 312 (1971).
- <sup>20</sup>D. O. Hebb, *The Organization of Behavior* (Wiley, New York, 1949).
- <sup>21</sup>R. Bellman and K. L. Cooke, *Differential-Difference Equations* (Academic, New York, 1963).
- <sup>22</sup>G. Toulouse, *Commun. Phys.* **2**, 115 (1977).
- <sup>23</sup>For a recent review of spin glasses, see K. Binder and A. P. Young, *Rev. Mod. Phys.* **58**, 801 (1986).
- <sup>24</sup>D. C. Mattis, *Phys. Lett.* **56A**, 421 (1976).
- <sup>25</sup>R. M. May, *Stability and Complexity in Model Ecosystems*, 2nd ed. (Princeton University Press, New Jersey, 1974).
- <sup>26</sup>W. Jeffrey and R. Rosner, *Ref. 1*, p. 241.
- <sup>27</sup>J. D. Reger and K. Binder, *Z. Phys. B* **60**, 137 (1985).
- <sup>28</sup>S. Amari, *Proc. IEEE* **59**, 35 (1971).
- <sup>29</sup>S. Shinomoto, *Prog. Theor. Phys.* **75**, 1313 (1986).
- <sup>30</sup>H. Gutfreund, J. D. Reger, and A. P. Young, *J. Phys. A* **21**, 2775 (1988).
- <sup>31</sup>K. E. Kürten, *Phys. Lett.* **129A**, 157 (1988).
- <sup>32</sup>S. Amari, *IEEE Trans. SMC-2*, 643 (1972).
- <sup>33</sup>K. E. Kürten and C. W. Clark, *Phys. Lett.* **114A**, 413 (1986).
- <sup>34</sup>H. Sompolinsky, A. Crisanti, and H. J. Sommers, *Phys. Rev. Lett.* **61**, 259 (1988).
- <sup>35</sup>M. Y. Choi and B. A. Huberman, *Phys. Rev. B* **31**, 2862 (1983).
- <sup>36</sup>E. P. Wigner, *Ann. Math.* **67**, 325 (1958).
- <sup>37</sup>S. F. Edwards and R. C. Jones, *J. Phys. A* **9**, 1595 (1976).
- <sup>38</sup>The eigenvalue spectrum for large asymmetric random matrices has recently been analyzed. H. J. Sommers, A. Crisanti, H. Sompolinsky, and Y. Stein, *Phys. Rev. Lett.* **60**, 1895 (1988).
- <sup>39</sup>At  $p_- = 1$  the result of Eq. (4.5) is used instead of Eq. (5.10) which neglects terms of  $O(1/N)$  and is not correct at  $p_- = 1$ .
- <sup>40</sup>D. J. Amit, H. Gutfreund, and H. Sompolinsky, *Phys. Rev. A* **32**, 1007 (1985).
- <sup>41</sup>J. S. Denker, *Ref. 1*, p. 121.